

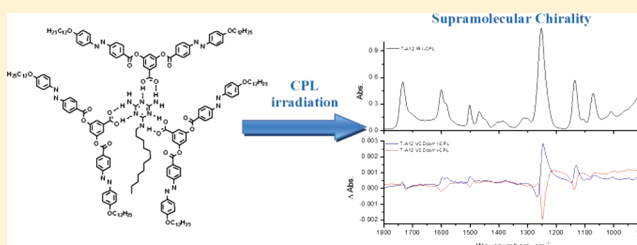
# Study of the Photoinduced Supramolecular Chirality in Columnar Liquid Crystals by Infrared and VCD Spectroscopies

Juan Ramón Avilés Moreno,<sup>†</sup> Juan Jesús López González,<sup>\*,†</sup> Francisco Partal Ureña,<sup>†</sup> Francisco Vera,<sup>‡</sup> M. Blanca Ros,<sup>‡</sup> and Teresa Sierra<sup>\*,‡</sup>

<sup>†</sup>Department of Physical and Analytical Chemistry, Experimental Sciences Faculty, University of Jaén, Campus Las Lagunillas, E-23071 Jaén, Spain

<sup>‡</sup>Instituto de Ciencia de Materiales de Aragón, Química Orgánica, Facultad de Ciencias, Universidad de Zaragoza-CSIC, 50009 Zaragoza, Spain

**ABSTRACT:** IR and VCD spectroscopies are employed to clarify the molecular origins of supramolecular chirality in azobenzene-containing columnar liquid crystals. The different columnar mesomorphic assemblies, Col<sub>r</sub> and Col<sub>h</sub>, of an achiral and a chiral propeller-like hydrogen-bonded complex, respectively, are used for this study. The mesomorphic behavior of the achiral complex is studied here for the first time, and the structural parameters of its Col<sub>r</sub> mesophase are determined by X-ray diffraction. Both complexes bear azobenzene units and this makes it possible to implement photoresponsive columnar architectures, the chirality of which can be induced and modulated by irradiation with 488 nm circularly polarized light (CPL). Thin films of the respective rectangular and hexagonal columnar phases of these complexes have been processed in order to study the IR absorption spectra and the vibrational circular dichroism responses upon irradiation with CPL. These studies allow confirming that the outer part of the columns, consisting on azobenzene groups, is mainly involved in the photoinduced supramolecular chirality, rather than the inner part of the columns where a melamine core is located. This supports a structural model based on the helical disposition of the azobenzene groups along the stacked propeller-like complexes.



## INTRODUCTION

Though vibrational circular dichroism (VCD) spectroscopy has been known since the 1970s,<sup>1–5</sup> it has been in the last 2 decades when this technique has taken a special relevance in the study of chiral chemical species and materials. In the decade of the 1990s, Stephens and co-workers<sup>6,7</sup> developed the theoretical framework that allows simulating the VCD spectra of enantiomers using quantum chemical calculations and the determination of absolute configurations<sup>8</sup> and conformational landscapes<sup>9–13</sup> of small molecules in solution. Also, the commercialization of VCD instruments in these 15 last years has allowed this technique to become available in an increasing number of laboratories worldwide.<sup>14–21</sup>

More recently, VCD spectroscopy has also been used as a powerful tool to obtain information about chiral induction in supramolecular organizations.<sup>20–24</sup> Thus, combined with other techniques, VCD spectroscopy was successfully used by us to propose a model of helical organization for a photoinduced supramolecular chiral architecture in the mesophase of a well characterized azopolymer.<sup>21</sup>

Circularly polarized light (CPL) is a chiral electromagnetic radiation that has been shown to be able to induce absolute asymmetric synthesis.<sup>25</sup> Photochromic liquid crystals appeared as attractive systems for the design of chiroptical switches based on supramolecular organizations interacting with CPL.<sup>26,27</sup> Azobenzene-containing liquid crystals, which have been widely

investigated due to their phototunable optical properties such as birefringence and dichroism,<sup>28–31</sup> have also been described to undergo chiral induction and/or chiral inversion effects through *E/Z* photoisomerization of azobenzene groups situated in the constituent mesogens. The photoinduced chiral organizations have been reported for calamitic mesophases, either nematic or smectic,<sup>32,33</sup> B-type mesophases<sup>34</sup> and columnar mesomorphic organizations.<sup>35</sup>

For nematic azopolymers, the use combined of IR and VCD spectroscopies allowed to observe that the “fingerprints” of the photoinduced chirality would be associated with its side-chain azobenzene moiety, arranged within a chiral nematic organization, and not to its methacrylate main chain adopting a one-sense helical conformation.<sup>21</sup>

VCD spectroscopy has proven to be a useful technique to study chiral columnar mesophases. In fact, it has been used to show that disk-like molecules with axial chirality segregate into chiral domains in the mesophase.<sup>36</sup> Further, the present work aims to get deep insight into the molecular origins of the chiral columnar organizations proposed for propeller-like H-bonded complexes,<sup>35a</sup> which undergo chiral photoresponse upon irradiation with CPL, by using IR and VCD techniques.

Received: February 22, 2012

Revised: March 21, 2012

Published: April 3, 2012

Our study is performed for a new achiral complex, T-A12 (Figure 1), and for a chiral complex, T-A(S)10\* previously

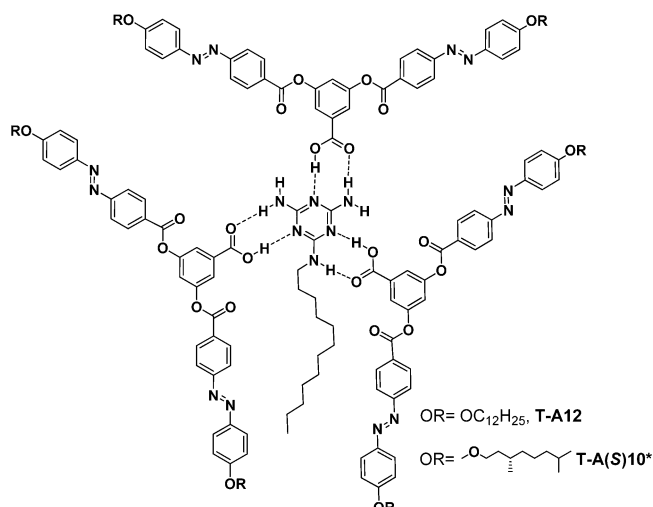


**Figure 1.** Structure of the hydrogen-bonded complexes T-A(S)10\* and T-A12.

described.<sup>35a</sup> T-A12 shows a rectangular columnar mesomorphic arrangement and T-A(S)10\* was reported to show a hexagonal columnar mesomorphic arrangement. The application of IR and VCD spectroscopies helps to determine the different participation of the molecular components in the photo-induced supramolecular chirality and, thus, to confirm that it is mainly associated with the helical arrangement of azobenzene groups in the periphery of the columns rather than to their inner melamine core.

## EXPERIMENTAL SECTION

The complex T-A12 was prepared by slow evaporation of a dichloromethane solution containing the melamine, T, and the acid, A12, respectively, in a 1:3 ratio. The synthesis of the V-shaped acid A12 was carried out following the procedure described in a previous work.<sup>35b</sup> The complex thus prepared was heated above the clearing point before used for further studies.

Variable temperature Infrared studies were performed on KBr pellets using a Nicolet Avatar 380-FTIR in the 4000–400 cm<sup>-1</sup> spectral region with a variable temperature system.

Thermal measurements were carried out by differential scanning calorimetry (DSC), performed with a DSC-MDSC TA Instruments Q-2000. Liquid crystal textures were studied using an Olympus BX-50 polarizing microscope equipped with a Linkam TMS91 hot stage and a CS196 hot-stage central processor. Microphotographs were taken with a digital camera Olympus DP12.

X-ray Diffraction measurements were carried out at room temperature using a Pinhole camera (Anton-Paar) operating with a point focused Ni-filtered Cu K $\alpha$  beam. The sample was held in Lindemann glass capillaries (1 mm diameter). The diffraction patterns were collected on a flat photographic film perpendicular to the X-ray beam.

Circular dichroism spectra (CD) were recorded in a Jasco J-810 for a l-CPL irradiated thin film with the 488 nm line of an Ar<sup>+</sup> laser (20 mW cm<sup>-2</sup>) for 30 min. The thin film was prepared by casting a solution of the complex in dichloromethane onto a quartz plate.

Infrared and VCD spectra of nonirradiated and l-CPL and r-CPL irradiated films (prepared on BaF<sub>2</sub> plates) from the 488 nm line of an Ar<sup>+</sup> laser (20 mW cm<sup>-2</sup>) for 30 min were recorded at a resolution of 4 cm<sup>-1</sup> in the 2000–900 region with a JASCO FVS-4000 spectrophotometer (4000 scans and 45 min of acquisition time).

In order to detect possible artifacts in both CD and VCD spectra, the recommendations of Shindo et al.<sup>37</sup> related to the

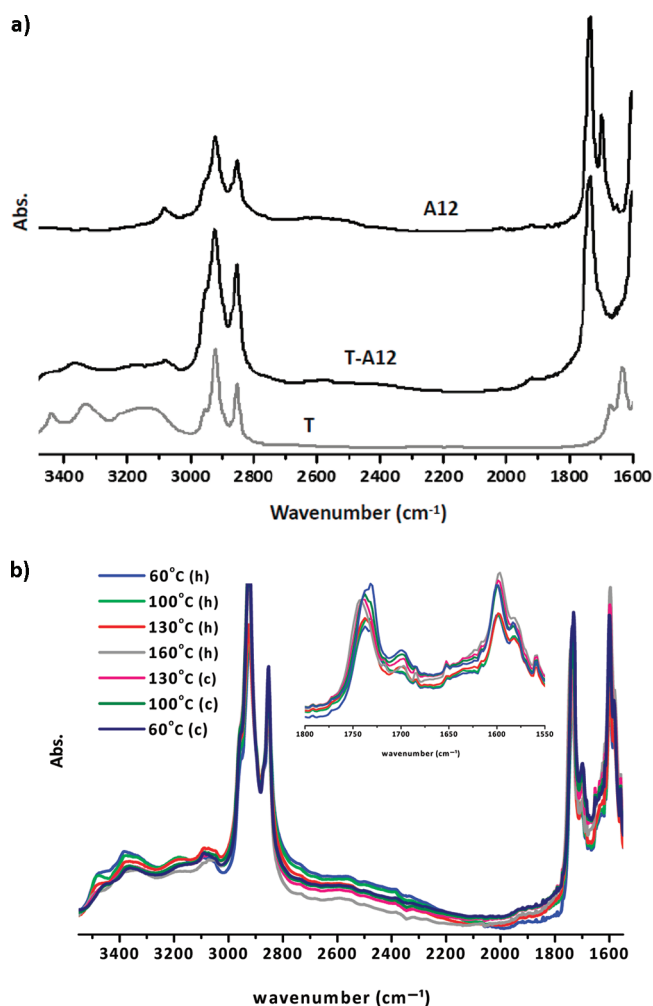


**Figure 2.** (a) IR spectra of T, A12 and T-A12 recorded on KBr pellets at room temperature. (b) IR spectra of T-A12 recorded on a KBr pellet at different temperatures in a heating (h)–cooling (c) cycle. A zoom in the 1800–1550 cm<sup>-1</sup> region is also shown.

**Table 1. Thermal Properties of the H-Bonded Complexes and Structural Parameters Measured by X-ray Diffraction at Room Temperature of the Respective Columnar Mesophases of T-A12 and T-A(S)10\***

	thermal properties T °C [ $\Delta H$ , kJ/mol]	lattice parameters	$d_{\text{obs}}$ (Å)	$d_{\text{calc}}$ (Å)	hk
T-A12	I 137.3 °C [1.8] Col <sub>r</sub>	$a = 94$ Å	53.0	52.9	11
		$b = 64$ Å	31.8	32.0	02
			15.7	16.0	04
T-A(S)10* <sup>35a</sup>	I 123 °C [2.0] Col <sub>h</sub> 51 °C g	$a = 65.2$ Å	56.4	56.5	10
		$h = 3.3$ Å	32.9	32.6	11
			21.3	21.3	21
			16.2	16.3	31

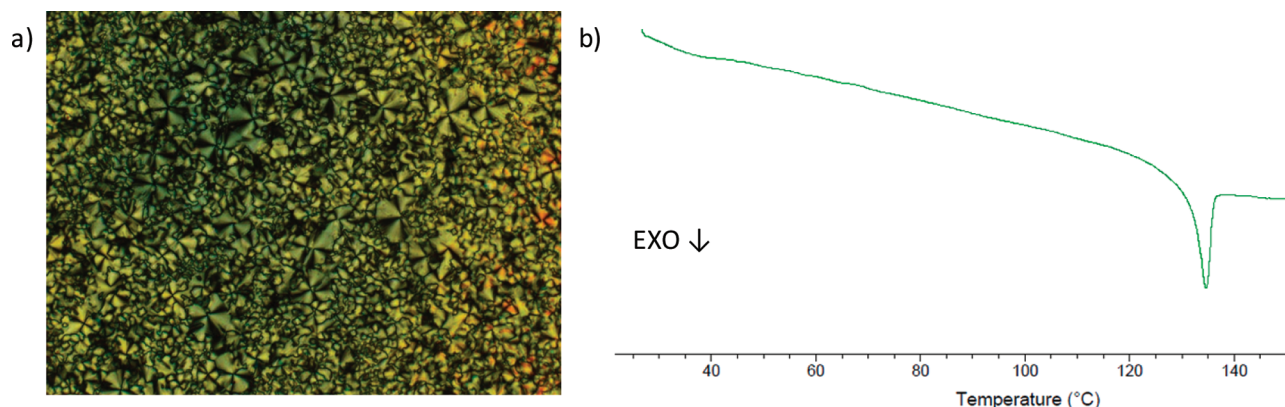


**Figure 3.** (a) POM photograph ( $\times 40$ ) of a film of T-A12 between glass slides. The crossed whit arrows indicate the position of the crossed polarizers. (b) DSC thermogram of complex T-A12 in the second cooling process (EXO down).

rotation of the samples were taken into account. Thus, the samples were rotated  $90^\circ$ ,  $180^\circ$ , and  $270^\circ$  around the beam propagation axis and  $180^\circ$  around the vertical axis, without changes in the observed spectra. The corrected VCD spectra were obtained by subtracting the VCD spectrum of the nonirradiated film to those of the l-CPL and r-CPL irradiated films.

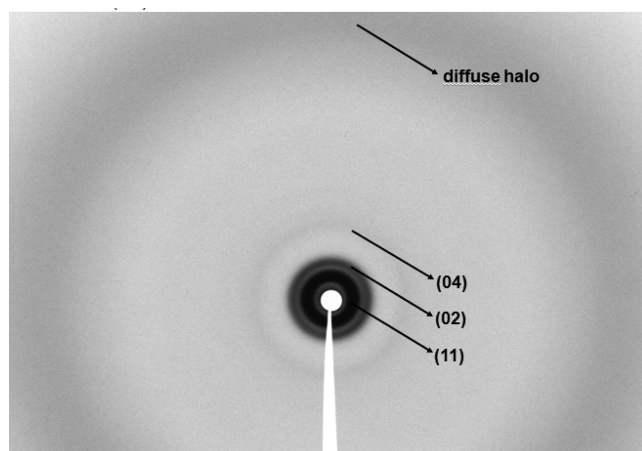


**Figure 4.** X-ray diffraction pattern of the complex T-A12 recorded at room temperature.

## RESULTS AND DISCUSSION

**IR Study of the Formation and Stability of the Hydrogen-Bonded Complexes.** The formation of the T-A12 complex as well as the stability of H-bonding interactions with temperature was studied by IR spectroscopy in neat samples as KBr pellets. Figure 2a shows a comparative between the IR spectra of the melamine, T, the V-shaped acid, A12, and the [1:3] complex, T-A12. The stretching C=O band corresponding to acid group appears at  $1698\text{ cm}^{-1}$  for the acid, A12, and corresponds to its cyclic dimeric form. For the complex, T-A12, this band shifts to lower wavelengths and appears as a shoulder of the stretching C=O band of the ester groups, at  $1705\text{ cm}^{-1}$ . This is consistent with the establishment of H-bonding interactions between the C=O group and the N-H groups of the melamine.<sup>38</sup>

The stability of the complex with temperature was studied by temperature dependent IR spectroscopy on KBr pellets. Figure 2b reflects the dynamic nature of hydrogen-bonding interactions when the spectra were recorded at different temperatures, up to  $160^\circ\text{C}$ . It is evident that characteristic bands related with H-bonding interactions changed in a reproducible manner according to the heating and cooling processes.

**Thermal properties.** T-A12 shows liquid crystalline behavior in a broad temperature interval. The study of T-A12 was performed with the usual techniques, i.e. polarized optical

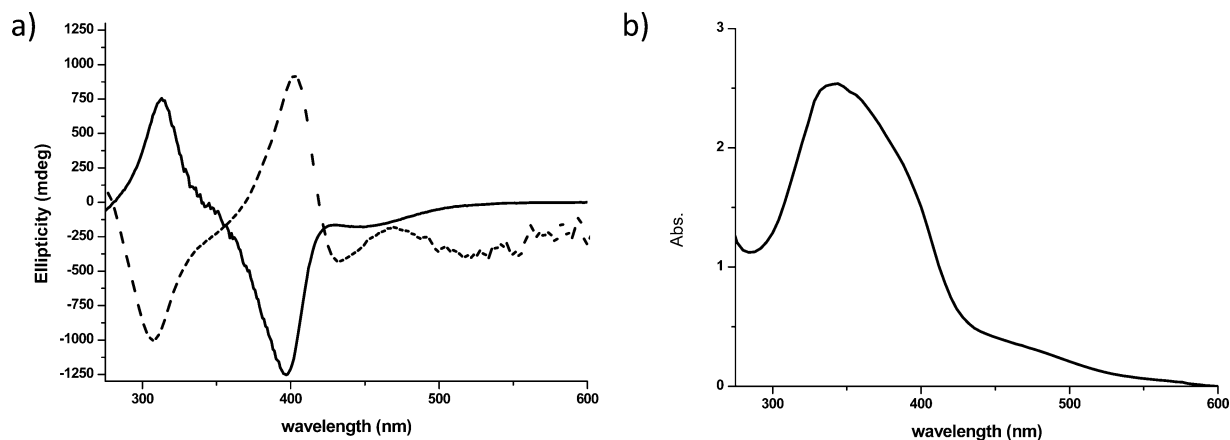


**Figure 5.** CD (a) and UV (b) spectra of T-A12 recorded for a thin film casted on a quartz plate and irradiated with left-handed (solid line) and right-handed (dashed line) CPL at room temperature.

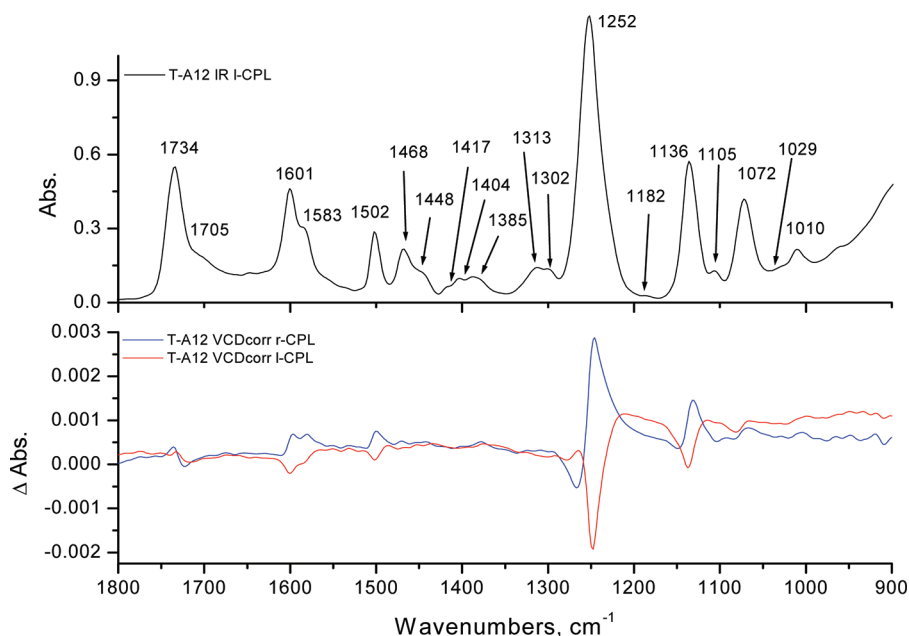


**Figure 6.** IR spectrum (top) and corrected VCD spectrum (bottom) of T-A12 in the 1800–1000  $\text{cm}^{-1}$  spectral region: r-CPL irradiated film (blue) and l-CPL irradiated film (red) for 30 min ( $20 \text{ mW cm}^{-1}$ ).

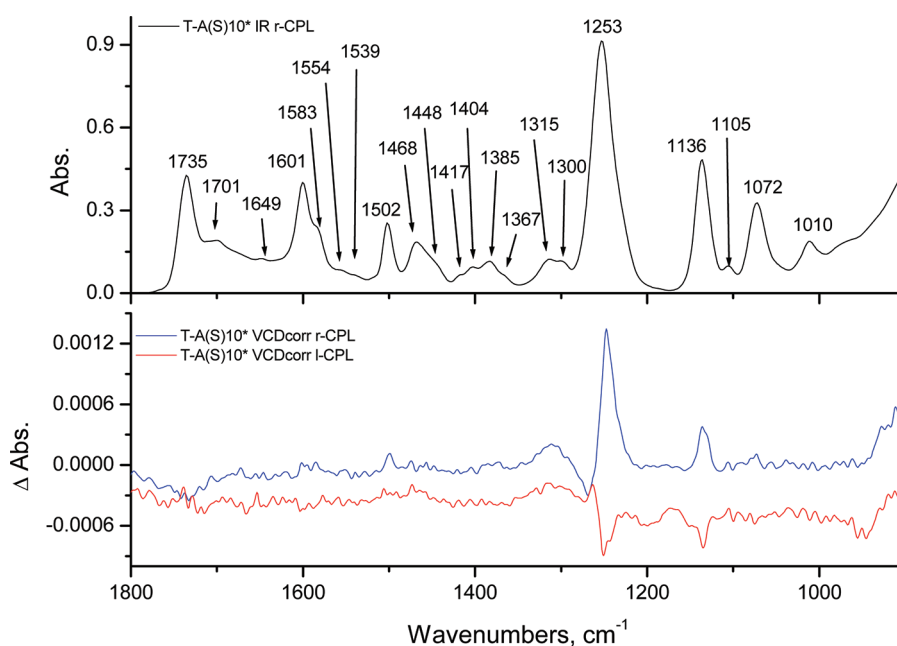


**Figure 7.** IR spectrum (top) and corrected VCD spectrum (bottom) of T-A(S)10\* in the 1800–1000  $\text{cm}^{-1}$  spectral region: r-CPL irradiated film (blue) and l-CPL irradiated film (red) for 30 min ( $20 \text{ mW cm}^{-1}$ ).

microscopy (POM), differential scanning calorimetry (DSC) and X-ray diffraction. The thermal data measured for T-A12 are included in Table 1 together with those already reported for T-A(S)10\*, for the sake of comparison.<sup>35a</sup>

T-A12 shows mesomorphic behavior, which is stable at room temperature for long periods of time. POM textures (Figure 3a) appeared as schlieren zones with Maltese crosses, which suggest the existence of a columnar mesomorphase. Moreover, the extinction brushes are inclined with respect to the direction of the crossed polarizers, indicating the presence of molecular tilt. This result led us to indentify the mesophase as  $\text{Col}_t$ ,<sup>39</sup> which is in contrast to the  $\text{Col}_h$  mesophase found for the chiral complex.

The DSC thermogram revealed only one peak in the cooling process (Figure 3b), which corresponds to the appearance of the mesophase from the isotropic liquid. Unlike the chiral complex, in which the mesomorphic order is frozen into a glassy state below  $T_g = 51^\circ\text{C}$ , a glass transition does not appear in the cooling scan. This indicates that the achiral complex maintains the liquid crystalline state at room temperature even though the viscosity of the mesophase is very high at this temperature.

Confirmation of the nature of the  $\text{Col}_t$  mesophase of T-A12, as it appears in Table 1, was achieved by X-ray diffraction experiments at room temperature, which also confirmed the



**Table 2.** IR Wavenumbers ( $\text{cm}^{-1}$ ) and VCD Main Features of T-A12 and T-A(S)10\* in the 1800–1000  $\text{cm}^{-1}$  Spectral Region and Assignment of the Observed Bands<sup>a</sup>

T-A12		T-A(S)10*		<i>E</i> -azobenzene and melamine bands	description
observed IR	rel intens	observed IR	rel intens		
1734	m	1735	m	—	aryl C=O str free (1740–1705 $\text{cm}^{-1}$ )
1705	w	1701	w	—	C=O str linked
—	—	1649	w	1653 (2, A <sub>1</sub> ', melamine)	NH str
1601	m	1601	m	1595 (6, Ag)	CC str, def ring
1583	m	1583	m	1591 (50, Bu)	CC str, def ring
—	—	1554	m	1586 (51, Bu)	ring str
—	—	1539	w	1563 (13, A <sub>2</sub> ', melamine)	—
1502	m	1502	m	1493 (9, Ag)	def CH <sub>ring</sub>
1468	m	1468	m	1484 (52, Bu)	def CH <sub>ring</sub> , CC str
1448	w	1448	w	1473 (10, Ag)	def CH <sub>ring</sub> , NN str
1417	w	1417	w	1454 (53, Bu)	def CH <sub>ring</sub>
1404	w	1404	w	1450 (14, E', melamine)	CN str
1385	w	1385	w	1443 (8, Ag)	NN str
—	—	1367	vw	1443 (3, A <sub>1</sub> ', melamine)	ring str + CN str
1313	w	1315	w	—	—
1302	w	1300	w	—	—
1252	s	1253	s	1379 (11, Ag)	CC str
1182	vw	—	—	1315 (12, Ag)	def CH <sub>ring</sub>
1136	m	1136	m	1307 (55, Bu)	def CH <sub>ring</sub>
1105	w	1105	w	1184 (13, Ag)	ArC—O—C—Alk str asym (1275–1200)
1072	m	1072	m	1181 (57, Bu)	def CH <sub>ring</sub> , def ring
1029	w	—	—	1158 (14, Ag)	def CH <sub>ring</sub>
1010	w	1010	w	1146 (15, Ag)	def CH <sub>ring</sub>
				1155 (58, Bu)	CN str, def CH <sub>ring</sub>
				1071 (16, Ag)	def CH <sub>ring</sub>
				1070 (59, Bu)	def CH <sub>ring</sub> , CC str
				1023 (17, Ag)	def CH <sub>ring</sub>
				1021 (60, Bu)	CC str, def CH <sub>ring</sub>
				1003 (18, Ag)	def CH <sub>ring</sub> , CC str
				1000 (61, Bu)	def ring

<sup>a</sup>Key: s = strong, m = medium, w = weak; str = stretching, def. = in-plane deformation, asym = asymmetric, Ar = aryl, Alk = alkyl.

stability of the mesophase order at ambient conditions. The lattice parameters *a* and *b* of the rectangular columnar arrangement were calculated from the diffraction maxima measured at low angles in the X-ray pattern (Figure 4). The outer maximum, which appears as a diffuse halo, corresponds to the molten aliphatic chains and is usually observed in liquid crystalline systems. The type of columnar mesophase shown by the achiral complex is, thus, different from the mesophase of the chiral complex T-A(S)10\*, which was identified as hexagonal columnar mesophase with long-range correlation stacking order (see data included in Table 1).<sup>35a</sup> From density estimations, the number of complexes per unit cell was found *Z* = 4 for the achiral complex. This value, and the *Z* = 2 value previously found for the hexagonal columnar mesophase of the chiral complex, are consistent with a bidimensional arrangement in which two complexes are located in each node of the corresponding lattice.<sup>35a,38</sup>

**Photoinduction and Photocontrol of Chirality. Electronic and Vibrational Circular Dichroism.** Following similar procedures previously described,<sup>35a</sup> we checked the photoresponse of the achiral complex to CPL. As expected, the as-prepared thin film of T-A12 on a quartz plate was CD silent.

However, it was possible to induce supramolecular chirality into the Col<sub>r</sub> mesophase of T-A12 by irradiation with CPL for 30 min at room temperature. Figure 5 shows the CD spectrum of a thin-film irradiated with l-CPL, which shows an intense exciton coupling centered at the maximum absorption wavelength of the azobenzene chromophore. This CD signal can be assigned to a helical disposition of chromophores. Accordingly, we can propose a helical arrangement of propeller-like complexes along the column, the sense of which is determined by the sign of the polarization of the radiation used.

In order to determine the origins of the helical arrangement and which parts of the H-bonded complexes are most affected by the induced supramolecular chirality, we undertook VCD studies on l-CPL and r-CPL irradiated films of both T-A12 and T-A(S)10\* complexes. VCD absorption signals of opposite sign in irradiated films of both complexes are only observed in the 1800–1000  $\text{cm}^{-1}$  region for the l-CPL and r-CPL irradiated films; the samples are VCD-silent prior to irradiation. IR and VCD spectra of irradiated T-A12 and T-A(S)10\* films are shown in Figures 6 and 7, respectively, and their data are gathered in Table 2. Wavenumber shifts in the VCD bands with respect to the IR ones are negligible.

Almost all the observed bands are associated with normal modes of azobenzene unit<sup>40</sup> except for the more intense couplet associated with the 1252 cm<sup>-1</sup> (T-A12) and 1253 cm<sup>-1</sup> (T-A(S)10\*) IR bands, which are assigned to the asymmetric stretching of the two (Ar)C–O–C(Alk) groups.<sup>41,42</sup> This band is an example to illustrate that from the VCD spectra of chiral systems often we can obtain more information than from the IR ones. In this case, only one absorption band is observed in the 1200–1280 cm<sup>-1</sup> region in the IR spectrum, involving two different normal modes. However, in the VCD spectra of T-A12 and T-A(S)10\* a couplet is observed, showing that this IR band is a complex one. The same can be applied to the IR absorption bands at 1601 and 1502 cm<sup>-1</sup> in the case of T-A12 complex. Each one of them is associated with two different normal modes and both correspond to complex signals in its VCD spectrum and very similar to those observed in P100 liquid crystal,<sup>21</sup> where well-defined couplets are observed. In the case of T-A(S)10\* complex, VCD signals are not observed for these IR bands at 1601 and 1502 cm<sup>-1</sup>.

On the contrary, the IR band at 1583 cm<sup>-1</sup> corresponding to only one normal mode for both complexes (T-A12 and T-A(S)10\*), assigned to the C=C stretching (and deformation of the aromatic rings), is observed also as a simple absorption band in the VCD spectrum, but only for T-A12 complex. In addition, the complex IR band at 1136 cm<sup>-1</sup>, assigned to the C–N stretching (and deformation of the aromatic CH), is observed as a VCD simple band for both T-A12 and T-A(S)10\* complexes.

Finally, bands of medium intensity at 1734 and 1735 cm<sup>-1</sup>, assigned to the C=O stretching of the ester groups of the central part of the V-shaped acids, appear in the IR spectrum of T-A12 and T-A(S)10\* without their corresponding counterparts in the respective VCD spectra of both samples. Likewise, IR bands that could be assigned to the melamine moieties at 1448 cm<sup>-1</sup> for the T-A12 and 1649, 1554, and 1448 cm<sup>-1</sup> for the T-A(S)10\*<sup>43</sup> do not present their counterparts in the VCD spectra. These findings show that only the 4-alkoxyazobenzene arms of the V-shaped acids are involved in the chiral supramolecular organization induced by CPL, and these groups are responsible for the chiroptical properties.

## CONCLUSIONS

An achiral complex prepared through H-bonding interactions between a melamine derivative and V-shaped acids in a ratio 1:3, respectively, is reported to show a rectangular columnar mesophase, Col<sub>r</sub>, which is stable at room temperature as demonstrated by POM, DSC and X-ray diffraction. Furthermore, it is possible to induce supramolecular chirality into the mesophase of this complex by irradiation with Circularly Polarized Light as confirmed by electronic and vibrational circular dichroism.

The combination of IR and VCD techniques turns to be a very useful tool for clarifying the contribution of the different molecular moieties to the photoinduced supramolecular chirality in two types of columnar mesophase, Col<sub>r</sub> and Col<sub>h</sub>, shown by the achiral H-bonded complex T-A12 and its chiral analogue, T-A(S)10\*,<sup>35a</sup> respectively. The comparison between the IR-VCD features of T-A(S)10\* and T-A12 and those of the previously studied azopolymer<sup>21</sup> results to be similar, which means that the supramolecular chiral architecture could have a common origin in their azobenzene groups. Thus, it is proposed that the outer part of the column is mainly involved in the photoinduced supramolecular chirality, rather than the inner part of the columns in which the melamine core is

located. This supports a model based on the helical disposition of the azobenzene arms of the V-shaped acid moieties along the stacked propeller-like complexes.

## AUTHOR INFORMATION

### Corresponding Author

\*(J.J.L.G.) Telephone: +34-953-212754. Fax: +34-953-212940. E-mail: jjlopez@ujaen.es. (T.S.) Telephone: +34-976-762276. Fax: +34-976-761209. E-mail: tsierra@unizar.es.

### Notes

The authors declare no competing financial interest.

## ACKNOWLEDGMENTS

J.R.A.M. expresses thanks to the Ministry of Education and Science of Spain for the Post-Doc Grant SB2006-0119 and to the Andalusia Government for the Post-Doc Grant P08-FQM-04096. F.V. thanks the MEC for a grant. The authors thank the University of Jaén and the Andalusia Government for financial support, the MICINN Project MAT2009-14636-C03-01, FEDER founding (EU), and the Aragon Government.

## REFERENCES

- (1) Hsu, E. C.; Holzwarth, G. J. *Chem. Phys.* **1973**, *59*, 4678–4685.
- (2) Holzwarth, G.; Hsu, E. C.; Mosher, H. S.; Faulkner, T. R.; Moscovitz, A. J. *Am. Chem. Soc.* **1974**, *96*, 251–252.
- (3) Nafie, L. A.; Cheng, J. C.; Stephens, P. J. *J. Am. Chem. Soc.* **1975**, *97*, 3842–3843.
- (4) Nafie, L. A.; Keiderling, T. A.; Stephens, P. J. *J. Am. Chem. Soc.* **1976**, *98*, 2715–2723.
- (5) Polavarapu, P. L. *Vibrational Spectra: Principles and Applications with Emphasis on Optical Activity*; Elsevier Science: Amsterdam, 1998; ISBN: 044489599X.
- (6) Cheeseman, J. R.; Frisch, M. J.; Devlin, F. J.; Stephens, P. J. *Chem. Phys. Lett.* **1996**, *252*, 211–220.
- (7) Stephens, P. J.; Ashvar, C. S.; Devlin, F. J.; Cheeseman, J. R.; Frisch, M. J. *Mol. Phys.* **1996**, *89*, 579–594.
- (8) Stephens, P. J.; Devlin, F. J.; Pan, J. J. *Chirality* **2008**, *20*, 643–663.
- (9) Partal Ureña, F.; Avilés Moreno, J. R.; López González, J. J. *J. Phys. Chem. A* **2008**, *112*, 7887–7893.
- (10) Avilés Moreno, J. R.; Partal Ureña, F.; López González, J. J. *Phys. Chem. Chem. Phys.* **2009**, *11*, 2459–2467.
- (11) Partal Ureña, F.; Avilés Moreno, J. R.; López González, J. J. *Tetrahedron: Asymmetry* **2009**, *20*, 89–97.
- (12) Avilés Moreno, J. R.; Partal Ureña, F.; López González, J. J. *Vib. Spectrosc.* **2009**, *51*, 318–325.
- (13) Avilés Moreno, J. R.; Partal Ureña, F.; López González, J. J. *Structural Chem.* **2011**, *22*, 67–76.
- (14) Shanmugam, G.; Polavarapu, P. L. *Biophys. Chem.* **2004**, *111*, 73–77.
- (15) Buffeteau, T.; Ducasse, L.; Poniman, L.; Delsuc, N.; Huc, I. *Chem. Commun.* **2006**, 2714–2716.
- (16) Deplazes, E.; van Bronswijk, W.; Zhu, F.; Barron, L. D.; Ma, S.; Nafie, L. A.; Jalkanen, K. J. *Theor. Chem. Acc.* **2008**, *119*, 155–176.
- (17) Hobro, A. J.; Rouhi, M.; Conn, G. L.; Blanch, E. W. *Vibr. Spectrosc.* **2008**, *48*, 37–43.
- (18) Emura, M.; Yaguchi, Y.; Nakahashi, A.; Sugimoto, D.; Miura, N.; Monde, K. *J. Agric. Food Chem.* **2009**, *57*, 9909–9915.
- (19) Abbate, S.; Lebon, F.; Longhi, G.; Fontana, F.; Caronna, T.; Lightner, D. A. *Phys. Chem. Chem. Phys.* **2009**, *11*, 9039–9043.
- (20) Sadlej, J.; Dobrowolski, J. C.; Rode, J. E. *Chem. Soc. Rev.* **2010**, *39*, 1478–1488.
- (21) Tejedor, R. M.; Oriol, L.; Serrano, J. L.; Partal Ureña, F.; López González, J. J. *Adv. Funct. Mater.* **2007**, *17*, 3486–3492.
- (22) Graus, S.; Tejedor, R. M.; Uriel, S.; Serrano, J. L.; Alkorta, I.; Elguero, J. J. *Am. Chem. Soc.* **2010**, *132*, 7862–7863.

- (23) Hartwig, A.; Mahato, T. K.; Kaese, T.; Wohrle, D. *Macromol. Chem. Phys.* **2005**, *206*, 1718–1730.
- (24) Tian, G.; Zhu, G. S.; Yang, X. Y.; Fang, Q. R.; Xue, M.; Sun, J. Y.; Wei, Y.; Qiu, S. L. *Chem. Commun.* **2005**, 1396–1398.
- (25) Rau, H. *Chiral Photochemistry*, Vol. 11, Marcel Dekker: New York, 2004.
- (26) Vera, F.; Serrano, J. L.; Sierra, T. *Chem. Soc. Rev.* **2009**, *38*, 781–796.
- (27) Pijper, D.; Jongejan, M. G. M.; Meetsmia, A.; Feringa, B. L. *J. Am. Chem. Soc.* **2008**, *130*, 4541–4552.
- (28) Hagen, R.; Bieringer, T. *Adv. Mater.* **2001**, *13*, 1805–1810.
- (29) Kumar, G. S.; Neckers, D. C. *Chem. Rev.* **1989**, *89*, 1915–1925.
- (30) Natansohn, A.; Rochon, P. *Chem. Rev.* **2002**, *102*, 4139–4175.
- (31) Viswanathan, N. K.; Kim, D. Y.; Bian, S. P.; Williams, J.; Liu, W.; Li, L.; Samuelson, L.; Kumar, J.; Tripathy, S. K. *J. Mater. Chem.* **1999**, *9*, 1941–1955.
- (32) (a) Hore, D. K.; Natansohn, A. L.; Rochon, P. L. *J. Phys. Chem. B* **2003**, *107*, 2506–2518. (b) Iftime, G.; Labarthe, F. L.; Natansohn, A.; Rochon, P. *J. Am. Chem. Soc.* **2000**, *122*, 12646–12650. (c) Tejedor, R. M.; Millaruelo, M.; Oriol, L.; Serrano, J. L.; Alcalá, R.; Rodríguez, F. J.; Villacampa, B. *J. Mater. Chem.* **2006**, *16*, 1674–1680. (d) Barberá, J.; Giorgini, L.; Paris, F.; Salatelli, E.; Tejedor, R. M.; Angiolini, L. *Chem.—Eur. J.* **2008**, *14*, 11209–11221. (e) Tejedor, R. M.; Vera, F.; Oriol, L.; Sierra, T.; Serrano, J. L. *Mol. Cryst. Liq. Cryst.* **2008**, *489*, 105–118. (f) Barrio, J. d.; Tejedor, R. M.; Chinelatto, L. S.; Sanchez, C.; Pinol, M.; Oriol, L. *J. Mater. Chem.* **2009**, *19*, 4922–4930. (g) del Barrio, J.; Tejedor, R. M.; Chinelatto, L. S.; Sánchez, C.; Pinol, M.; Oriol, L. *Chem. Mater.* **2009**, *22*, 1714–1723. (h) Tejedor, R. M.; Serrano, J.-L.; Oriol, L. *Eur. Polym. J.* **2009**, *45*, 2564–2571.
- (33) Choi, S.-W.; Kawauchi, S.; Ha, N. Y.; Takezoe, H. *Phys. Chem. Chem. Phys.* **2007**, *9*, 3671–3682.
- (34) Choi, S.-W.; Izumi, T.; Hoshino, Y.; Takanishi, Y.; Ishikawa, K.; Watanabe, J.; Takezoe, H. *Angew. Chem., Int. Ed.* **2006**, *45*, 1382–1385.
- (35) (a) Vera, F.; Tejedor, R. M.; Romero, P.; Barberá, J.; Ros, M. B.; Serrano, J. L.; Sierra, T. *Angew. Chem., Int. Ed.* **2007**, *46*, 1873–1877. (b) Vera, F.; Barberá, J.; Romero, P.; Serrano, J. L.; Ros, M. B.; Sierra, T. *Angew. Chem., Int. Ed.* **2010**, *49*, 4910–4914.
- (36) Nagayama, H.; Varshney, S. K.; Goto, M.; Araoka, F.; Ishikawa, K.; Prasad, V.; Takezoe, H. *Angew. Chem., Int. Ed.* **2010**, *49*, 445–448.
- (37) Kuroda, R.; Harada, T.; Shindo, Y. *Rev. Sci. Instrum.* **2004**, *72*, 3802–3810.
- (38) Barberá, J.; Puig, L.; Romero, P.; Serrano, J. L.; Sierra, T. *J. Am. Chem. Soc.* **2006**, *128*, 4487–4492.
- (39) Barberá, J.; Iglesias, R.; Serrano, J. L.; Sierra, T.; de la Fuente, M. R.; Palacios, B.; Pérez-Jubindo, M. A.; Vázquez, J. T. *J. Am. Chem. Soc.* **1998**, *120*, 2908–2918.
- (40) Biswas, N.; Umapathy, S. *J. Phys. Chem. A* **1997**, *101*, 5555–5566.
- (41) Socrates, G. *Infrared Characteristics Group Frequencies. Tables and Charts*, 2nd ed.; Wiley: Chichester, U.K., 1994.
- (42) Buffeteau, T.; Natansohn, A.; Rochon, P.; Pezolet, M. *Macromolecules* **1996**, *29*, 8783–8790.
- (43) Fernández-Liencre, M. P.; Navarro, A.; López-González, J. J.; Fernández-Gómez, M.; Tomkinson, J.; Kearley, G. *J. Chem. Phys.* **2001**, *266*, 1–17.